

STRUCTURE AND ACIDITY MODIFICATION OF MORDENITE THROUGH ISOMORPHOUS Fe SUBSTITUTION

Geon Joong Kim and Wha Seung Ahn*

Department of Chemical Engineering, College of Engineering, Inha Univ., Incheon 402-751, Korea

(Received 17 October 1991 • accepted 17 April 1992)

Abstract—A series of Fe-modified mordenite were hydrothermally synthesized. The effects of substrate composition, aging time, reaction temperature, and reaction time upon the crystallization of the mordenite were investigated. Isomorphous substitution of Fe was confirmed by FT-IR and EPR analysis. Acid strength and acid sites distribution of each catalyst were measured by pyridine TPD, which showed that the number of strong acid sites in H-Fe-mordenite are smaller than in H-Al-mordenite. Structural characteristics and thermal stability were also examined using XRD, SEM and TG. Fe-substitution into the mordenite structure have resulted in substantial decrease in thermal stability. H-Fe-mordenite catalysts showed high selectivity towards p-xylene in toluene alkylation and in xylene isomerization reaction, compared with those obtained using H-Al-mordenite because of lower concentration of strong acid sites. In addition, these H-Fe-modified mordenite showed little hexane cracking activity. Deactivation in both toluene alkylation and xylene isomerization reaction and coke formation over H-Fe-mordenite in these reactions were negligible.

INTRODUCTION

Isomorphous substitution of Fe into the framework of zeolite would cause changes in acidity and to some extents modification in structure, altering the products selectivity as a result [1]. Trace amounts of non-framework Fe in the zeolites has also been shown to contribute to the overall catalytic activity [2]. Chu et al. [3] and Caris et al. [4] have reported on synthesis and characterization of Fe⁺³ substituted ZSM-5 using Mössbauer spectroscopy. Other Fe⁺³ substituted zeolites have been studied by Derouane et al. [5], Wichterlova [6], and by Bart et al. [7]. McNicol and Pott [8] have shown the existence of Fe⁺³ impurity in the Faujasite and mordenite framework using ESR, phosphorescence and chemical studies. Even though successful and consistent crystallization of a pure Fe-silicate analog of ZSM-5 has been relatively well established, the attempts to incorporate Fe⁺³ into the mordenite in sodium media have generally been unsuccessful [9]. Studies on the synthesis of Fe modified mordenite and determining its physico-chemical properties are very limited and, for this matter, the recent work by Chandwadkar et al. [10] is worth mentioning. In this work, we have studied the crystallization kinet-

ics of mordenite type zeolite containing Fe⁺³. Its thermal stability as well as catalytic activities in toluene alkylation and xylene isomerization reactions were also examined.

EXPERIMENTAL

Reaction mixtures were prepared from fine amorphous silica powders (Zeosil 77® from KoFran Co.), sodium aluminate (Junsei), sodium hydroxide (Junsei), FeCl₃·6H₂O (Kanto), and distilled water.

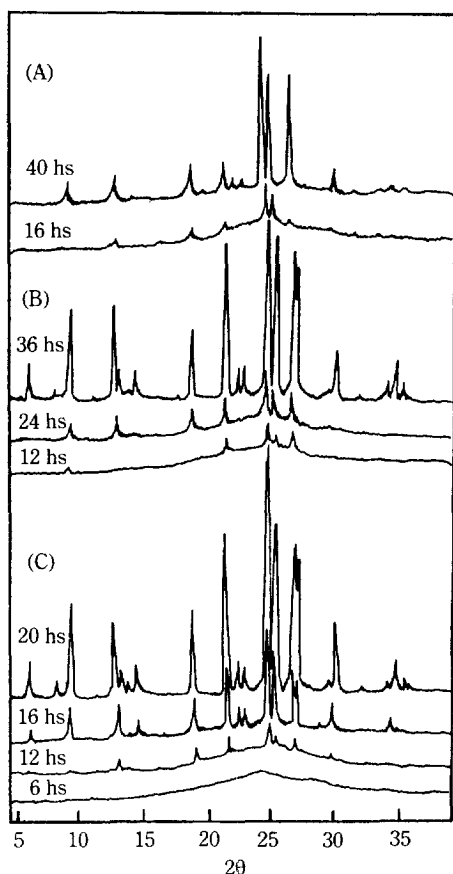
The reaction mixture was stirred thoroughly for 30 min and transferred to a 100 ml capacity stainless steel vessel in which hydrothermal reaction was carried out at 150-170°C without agitation. The substrate composition ranges expressed as oxides mole ratios were shown in Table 1. Samples were taken periodically and the solid products were washed with distilled water, filtered and dried at 120°C for 12 h. Its crystalline phase was identified using XRD (Philips, PW-1700, CuK α , Ni-filter) and the relative crystallinity of samples were determined by comparing the peak areas of the sample with those of the best crystallized mordenite.

Morphologies of the mordenites were examined using Scanning Electron Microscopy (Hitachi, X-650) and IR spectra were obtained with Nicolet 10 MX FT-

*To whom all correspondences should be addressed.

Table 1. Compositions of reactant mixtures for the synthesis of Fe-mordenite type zeolite

Run no.	Batch composition
1	2 Na ₂ O-Al ₂ O ₃ -10 SiO ₂ -0.1 Fe ₂ O ₃ -(200-260) H ₂ O
2	4 Na ₂ O-Al ₂ O ₃ -20 SiO ₂ -(0.1-0.2) Fe ₂ O ₃ -(400-520) H ₂ O
3	4 Na ₂ O-Al ₂ O ₃ -20 SiO ₂ -0.04 Fe ₂ O ₃ -520 H ₂ O
4	(4-6) Na ₂ O-Al ₂ O ₃ -20 SiO ₂ -0.067 Fe ₂ O ₃ -(520-780) H ₂ O
5	6 Na ₂ O-Al ₂ O ₃ -30 SiO ₂ -0.3 Fe ₂ O ₃ -(600-720) H ₂ O
6	8 Na ₂ O-Al ₂ O ₃ -40 SiO ₂ -0.4 Fe ₂ O ₃ -(800-960) H ₂ O
7	0.2 Na ₂ O-SiO ₂ -(0.03-0.5) Fe ₂ O ₃ -46 H ₂ O

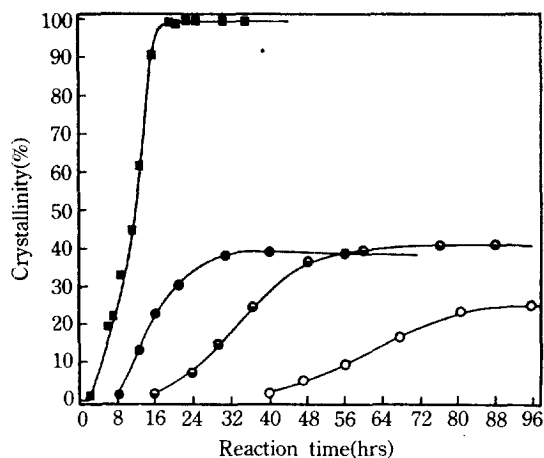
**Fig. 1. X-ray diffractograms of Al-mordenite and Fe modified mordenites with reaction time.**

(A) Al free Fe-mordenite synthesized from the composition of 0.2Na₂O-SiO₂-0.025Fe₂O₃-46H₂O

(B) Fe, Al-mordenite from 6Na₂O-Al₂O₃-30SiO₂-0.3 Fe₂O₃-780H₂O

(C) Al-mordenite from 6Na₂O-Al₂O₃-30SiO₂-780H₂O
No aging, Reaction temp.: 170°C

IR spectrometer. Electron paramagnetic resonance measurements were made on a Bruker spectrometer in

**Fig. 2. Effect of reaction temperature and aging time on the crystallization rate of Al free Fe-mordenite.**

Substrate composition: 0.2Na₂O-SiO₂-0.025Fe₂O₃-46H₂O(○●), 6Na₂O-Al₂O₃-30SiO₂-780H₂O(■)
No aging(○●), Aging 1 day at 30°C(●)
Reaction temp.: 150°C(○), 170°C(●●■)

the temperature range of 110 K-473 K.

Thermal stability and structural change of the Fe-mordenite were examined using DTA and XRD after calcination at 700-1000°C.

Catalytic activities of the H type mordenites for toluene alkylation with methanol and xylene isomerization reaction were measured in a fixed bed reactor at atmospheric pressure. Reaction products were analysed using gas chromatography(Hitachi 263-30, TCD) equipped with a SE-30 column.

RESULTS AND DISCUSSION

1. Synthesis of Fe-Mordenite

Typical XRD patterns of Al free Fe-mordenite-like phase(A), partially Fe substituted mordenites(B), and normal Al-mordenite are shown in Fig. 1. The Fe substituted mordenites(A and B) have essentially the same XRD pattern and the framework structure to typical Al-Mordenite(C). The XRD pattern of (A) was obtained from the aluminum-free substrate composition of 0.2 Na₂O-SiO₂-0.025 Fe₂O₃-46 H₂O, and the characteristic mordenite peaks at $d = 9.06, 6.51, 4.48, 3.95, 3.44, 3.36 \text{ \AA}$ indicate that Fe-O-Si bond only can construct the building unit of mordenite type zeolite phase.

Crystallization curves for Al free Fe-mordenite synthesized at 150 and 170°C, and a typical crystallization curve for Al-mordenite are shown in Fig. 2. Increases in reaction temperature were accompanied by decreases

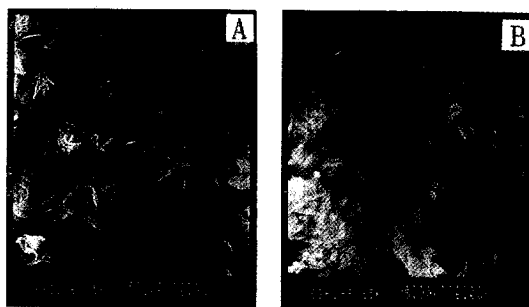


Fig. 3. Scanning electron micrographs of Al free modified mordenites.

Substrate composition: $0.2\text{Na}_2\text{O}\cdot\text{SiO}_2\cdot 0.025\text{Fe}_2\text{O}_3\cdot 46\text{H}_2\text{O}$, Reaction temp.: 170°C , Reaction time: 11hs (A), 48hs(B)

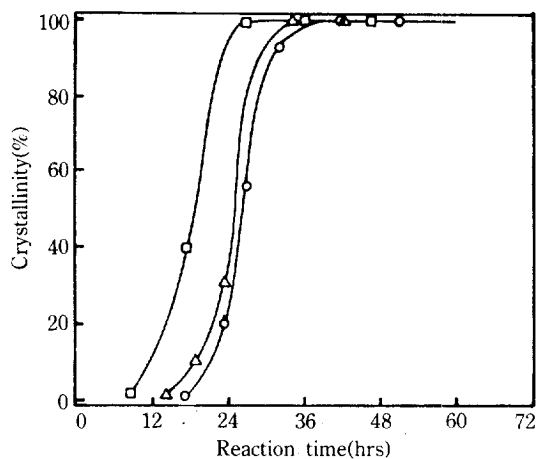


Fig. 4. Effect of $\text{SiO}_2/\text{Fe}_2\text{O}_3$ ratio on partially Fe-substituted mordenite crystallization rates.

Substrate composition: $\text{Na}_2\text{O}/\text{SiO}_2 = 0.2$, $\text{H}_2\text{O}/\text{Na}_2\text{O} = 130$, $\text{SiO}_2/\text{Al}_2\text{O}_3 = 20$, $\text{SiO}_2/\text{Fe}_2\text{O}_3 = 100(\circ)$, $300(\triangle)$, $500(\square)$, $1000(\diamond)$, Reaction temp.: 170°C

es in induction period and overall crystallization rates increased concurrently. The maximum crystallinity of the Al free Fe-mordenite was ca. 40%. Feasible reactant composition ranges for this Fe-mordenite were very narrow, and much α -Quartz were found co-produced.

In our earlier study on Al-mordenite synthesis [11], aging treatment at room temperature was found to have an adverse effect on crystallization rates and progressively larger crystals were obtained as the aging time was extended. On the other hand, in the Al free Fe-mordenite case, the rates of crystallization were slightly increased after 1 day aging. This Al free

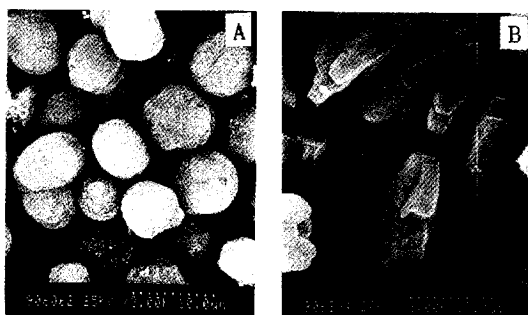


Fig. 5. Scanning electron micrographs of various Fe modified mordenite obtained from different reaction mixtures.

(A) $2\text{Na}_2\text{O}\cdot\text{Al}_2\text{O}_3\cdot 10\text{SiO}_2\cdot 0.1\text{Fe}_2\text{O}_3\cdot 260\text{H}_2\text{O}$
 (B) $6\text{Na}_2\text{O}\cdot\text{Al}_2\text{O}_3\cdot 20\text{SiO}_2\cdot 0.1\text{Fe}_2\text{O}_3\cdot 780\text{H}_2\text{O}$
 Reaction temp.: 170°C

Fe-mordenite was formed as agglomerated thin plate-shaped crystals as shown in Fig. 3.

The influence of $\text{SiO}_2/\text{Fe}_2\text{O}_3$ ratios of a starting mixture on the crystallization rates of partially Fe-substituted mordenite is shown in Fig. 4. The crystallization kinetics of Fe-mordenite showed virtually identical trends as those of the Al-mordenite (Fig. 2), and crystallization rates improved substantially with higher $\text{SiO}_2/\text{Fe}_2\text{O}_3$ ratios at constant $\text{SiO}_2/\text{Al}_2\text{O}_3$, $\text{Na}_2\text{O}/\text{SiO}_2$, and $\text{H}_2\text{O}/\text{Na}_2\text{O}$ ratios. It was also observed that addition of $\text{FeCl}_3\cdot 6\text{H}_2\text{O}$ to the substrate caused decreases in pH and resulted in hindering the crystallization rates. Samples with the substrate composition of $\text{SiO}_2/\text{Fe}_2\text{O}_3 = 100$ ($\text{SiO}_2/\text{Al}_2\text{O}_3 = 10$ or 20) has a light brown color, while Fe-mordenites prepared with $\text{SiO}_2/\text{Fe}_2\text{O}_3$ ratios down to 500 in the starting mixtures and dried at 120°C were completely white. Thus Fe-oxides were suspected to exist within the mordenite pores at high Fe_2O_3 concentrations.

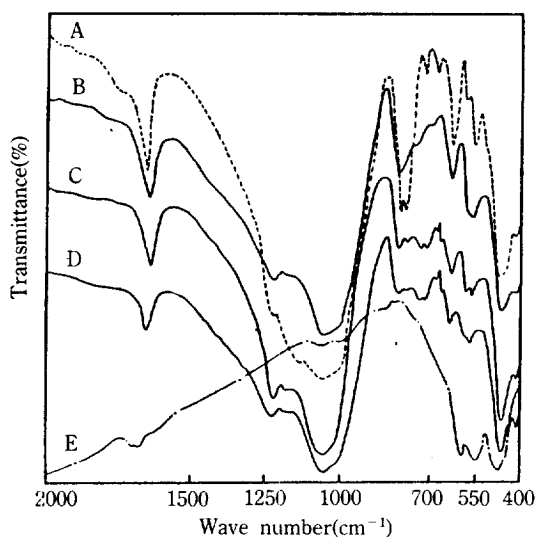
Fig. 5 shows the morphology of the Fe-mordenite crystals. Fe-mordenite with $\text{SiO}_2/\text{Al}_2\text{O}_3$ ratio of 10(A) showed spherical shape with average dimension of 5-7 μm , and larger disc-shaped crystals with corrosive surface were obtained with $\text{SiO}_2/\text{Al}_2\text{O}_3$ ratio of 20(B).

Chemical compositions and BET surface areas of the Fe-mordenites are summarized in Table 2. Possible extra-framework amorphous iron oxides were removed by HCl leaching for 30 min at 100°C . Relative crystallinity of the samples were maintained even after the acid treatment except for the Al free Fe-mordenite. Light brown color of the relatively Fe-rich mordenite samples disappeared as Fe is leached out, and their BET surface area increased considerably. On the other hand, Fe contents before and after ion-exchange

Table 2. Composition and surface area of Fe-mordenites

Sample no.	Mole ratio of substrate		Mole ratio of the as-synthesized mordenite		BET surface area (m ² /g)	BET area after 1N-HCl treatment (m ² /g)
	SiO ₂ /Al ₂ O ₃	SiO ₂ /Fe ₂ O ₃	SiO ₂			
			Al ₂ O ₃ +Fe ₂ O ₃	SiO ₂ /Fe ₂ O ₃		
1*	∞	30	26.4	26.4	146	collapse of structure
2	10	100	9.8	43.6	207	524
3	30	100	20.8	61.5	291	588
4	20	300	17.4	62.3	219	559

*Al free Fe-mordenite

**Fig. 6. IR spectra of Fe-mordenites, Al-mordenite and Fe₂O₃ powder.**

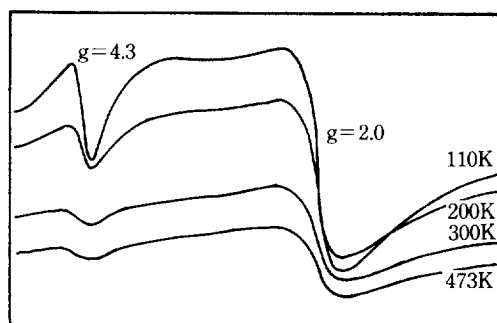
- A: Al free Fe-mordenite (sample 1)
 B: Al-mordenite (SiO₂/Al₂O₃ = 11.6)
 C: Fe-mordenite (sample 3)
 D: Fe-mordenite (sample 4)
 E: Fe₂O₃ powder

See Table 2 for the sample composition.

with NH₄⁺ ion, remained relatively constant. These evidences indicate that most Fe³⁺ in the Fe-mordenite are present at non-exchangeable framework positions in the mordenite, with some occlusion of Fe oxides in the pore channels.

2. Spectroscopic Investigation

IR spectra of normal Al-mordenite, Al free Fe-mordenite, partially Fe-substituted mordenite, and Fe₂O₃ powder are shown in Fig. 6. IR spectra of mordenites are known to show typical absorption bands at 450 cm⁻¹ (T-O bond), 560 and 580 cm⁻¹ (double ring), 720 and 800 cm⁻¹ (symmetric stretch), and 1045 and 1223 cm⁻¹ (asymmetric stretch) [2]. The absorption bands

**Fig. 7. EPR spectra of partially Fe-substituted mordenites as-synthesized form.**Modulator gain: 1.25 × 10⁴

are observed at near 560 cm⁻¹ for the mordenite family due to 5-3 member ring blocks [12]. Al free Fe-mordenite (A) has a characteristic infrared pattern of mordenite at around 1230 cm⁻¹, 1050 cm⁻¹, 800 cm⁻¹, 590 cm⁻¹, 560 cm⁻¹, and 460 cm⁻¹ and these bands are significantly different from the band pattern of Fe₂O₃ oxide. Partially Fe-substituted mordenites (C, D) also showed a pattern similar to the normal Al-mordenite (B), and Si-O-Fe bond vibrations could be found at near 690 cm⁻¹. Szostak and Thomas [13] have found that Si-O-Si symmetric stretch appeared at 768 cm⁻¹ and Si-O-Fe symmetric stretch occurred at 679 cm⁻¹ in the sodalite system.

EPR spectra of the Fe-mordenite are shown in Fig. 7. The EPR spectra of the synthesized Fe-mordenite had two resonance signals at g=4.3 and 2.0. Many authors [4, 6, 8, 13-16] have reported that the EPR signals at g=4.3 can be interpreted as Fe³⁺ lattice ions present in the tetrahedral coordination and their presence in the EPR spectra strongly supports the fact that Fe³⁺ are present in the zeolite framework. Signals near g=2.10 is usually assigned to Fe³⁺ ions in the Fe₂O₃ phase occluded in zeolite in octahedral oxygen coordination [6].

3. Thermoanalytical Investigations

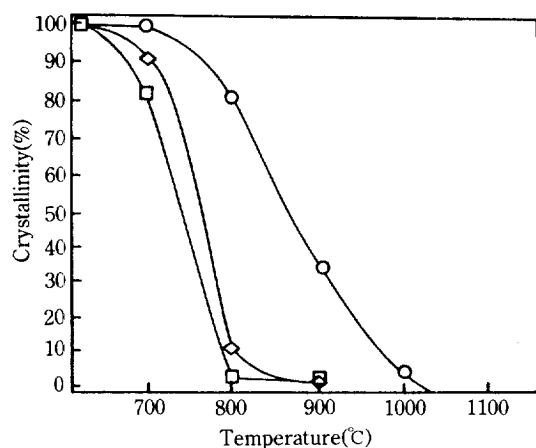


Fig. 8. Thermal stability of various mordenites.

Composition of mordenite: ○($\text{SiO}_2/\text{Al}_2\text{O}_3=11.6$, Al-mordenite), □(sample 3), ◇(sample 4). See Table 2 for the sample composition.

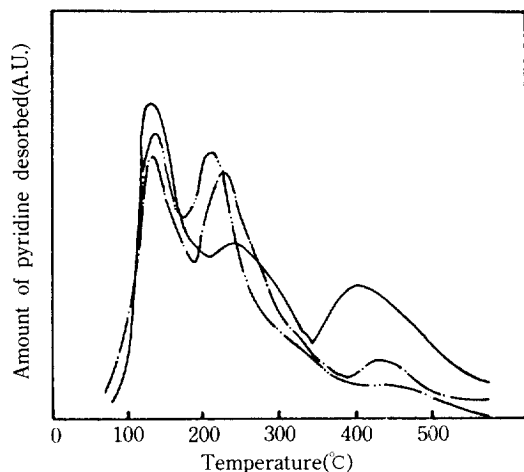


Fig. 9. Temperature programmed desorption of pyridine from various H type mordenites.

pyridine initially adsorbed at 100°C
 — $\text{SiO}_2/\text{Al}_2\text{O}_3=11.6$ (Al-mordenite)
 - - - sample 3
 ··· sample 4

See Table 2 for the sample composition.

Thermal stability of the Fe-modified mordenites under various calcination conditions were examined in Fig. 8. Even though the typical mordenite peaks were retained up to 700°C, Fe substitution into the mordenite structure in general have resulted in a substantial decrease in thermal stability compared with the normal Al-mordenite. This decrease in thermal

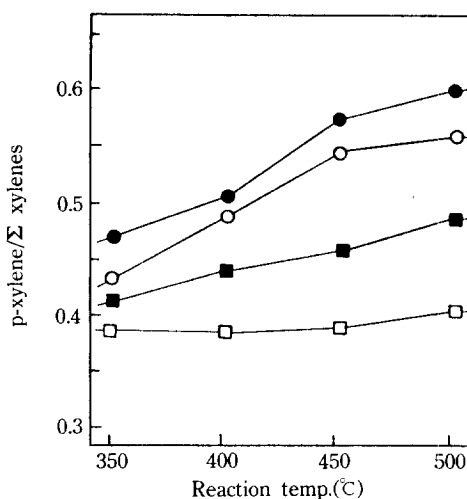


Fig. 10. Selectivity to p-xylene in toluene alkylation with methanol over various H type mordenite catalysts. toluene/methanol mol. ratio=2, WHSV=2.9h⁻¹ Catalyst composition: □($\text{SiO}_2/\text{Al}_2\text{O}_3=11.6$, Al-mordenite), ■($\text{SiO}_2/\text{Al}_2\text{O}_3=26.7$, Al-mordenite), ○(sample 3), ●(sample 4), See Table 2 for the sample composition.

stability for Fe-mordenite provides an additional evidence of isomorphous substitution of Fe into the mordenite framework(bond distances are Al-O=1.74 Å, Fe-O=1.84 Å, Si-O=1.60 Å) [16, 17].

4. TPD of Pyridine & Catalytic Activity

Results of pyridine TPD for H-Fe-mordenites and H-Al-mordenite($\text{SiO}_2/\text{Al}_2\text{O}_3=11.6$) are shown in Fig. 9. It is evident that H-Fe-mordenite has acidic sites distribution similar to those present in H-Al-mordenite. However, when Fe⁻³ ions were introduced into the mordenite framework, significant reduction in the peak area around 400°C was observed as compared with H-Al-mordenite, which indicates that the number of strong acid sites in H-Fe-mordenite are smaller than in H-Al-mordenite. On the other hand, acid sites with moderate acid strength seem to be increased with Fe introduction, as can be seen from the increase in the peak area around 200°C.

Catalytic activities of H-Fe-mordenites synthesized in this experiment were examined in the vapor phase toluene alkylation with methanol under atmospheric pressure. Fig. 10 shows that p-xylene fraction in the product increases with increasing reaction temperature, and the selectivity to p-xylene was improved markedly over H-Fe-mordenite. This improvement in p-xylene selectivity is believed to result from weakening of the original catalyst acidity by incorporating Fe³⁺

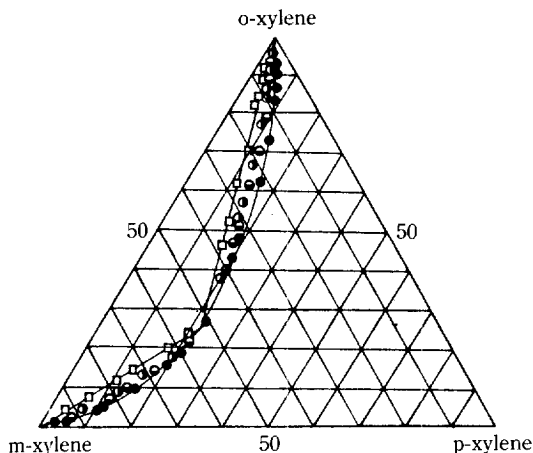


Fig. 11. Reaction paths for isomerization of pure xylene isomers over Fe modified H type mordenite catalysts.

WHSV: 24h^{-1} , reaction temp.: 350°C

□($\text{SiO}_2/\text{Al}_2\text{O}_3=11.6$, Al-mordenite), ●(sample 1), ◐(sample 3), ◑(sample 4). See Table 2 for the sample composition

into the lattice sites of the mordenite. Fe(III) oxides, precipitated inside the zeolite pores, might have also contributed towards steric hindrance to diffusion of various isomers and resulted in the high p-xylene selectivity.

Fig. 11 shows the composition of xylene isomers obtained in the isomerization reaction of pure xylene isomers over H-Fe-mordenite catalysts. For these catalysts, undesirable disproportionation reaction lowering the selectivity to p-xylene was negligible. Benzene, toluene and trimethylbenzenes in the products were quite small, and the higher para-selectivity was observed as compared with H-Al-mordenite catalyst. In addition, these Fe-modified mordenite type zeolite showed little hexane cracking activity. In both toluene alkylation and xylene isomerization reaction experiments, deactivation and coke formation over H-Fe-mordenites were negligible and more suppressed than with H-Al-mordenite. This information again indicates that Fe modification to the original mordenite has resulted in decrease in acid strength.

CONCLUSIONS

Fe substituted mordenite type zeolites were hydrothermally synthesized from the $\text{Na}_2\text{O}-\text{Al}_2\text{O}_3$ (or Al free) $-\text{SiO}_2-\text{Fe}_2\text{O}_3-\text{H}_2\text{O}$ system at $150-170^\circ\text{C}$, and their structural characteristics were investigated using various instrumental techniques. The combined results of IR

and EPR spectra, thermal stability, and the differences in the acidity shown by TPD were indicative of isomorphous substitution of Fe^{+3} ion into the zeolite lattice sites. H-Fe-mordenite catalysts showed high selectivity towards p-xylene in toluene alkylation and in xylene isomerization reaction, compared with those obtained using H-Al-mordenite because of lower concentration of strong acid sites. In addition, Fe_2O_3 impurities present in the pores might have contributed to the steric hindrance, resulting in high para-selectivity.

ACKNOWLEDGEMENT

This paper was supported by NON DIRECTED RESEARCH FUND, Korea Research Foundation, 1990.

REFERENCES

1. Tielen, M., Geelen, N. and Jacobs, P. A.: *Acta. Phys. Chem.*, **31**, 1 (1985).
2. Szostak, R.: "Molecular Sieves Principles of Synthesis and Identification", Van Nostrand Reinhold, New York, p. 317 (1989).
3. Chu, C. T. and Chang, C. D.: *J. Phys. Chem.*, **89**, 1569 (1985).
4. Calis, C., Frenken, P., deBoer, E., Swolfs, A. and Hefni, M. A.: *Zeolites*, **7**, 319 (1987).
5. Derouane, E. G., Mestdagh, M. and Vielvoye, L.: "Proceedings of the 3rd International Conference on Molecular Sieves", Zurich, p. 337 (1973).
6. Wichterlova, B.: *Zeolites*, **1**, 181 (1981).
7. Bart, J. C. J., Buriesci, N., Cariati, F., Petrer, M. and Zipelli, C.: *Zeolites*, **3**, 226 (1983).
8. McNicol, B. D. and Pott, G. T.: *J. of Catal.*, **25**, 223 (1972).
9. Bychkov, A. M., Polosin, A. V. and Senderov, E. E.: *Geochemistry*, 1799 (1987).
10. Chandwadkar, A. J., Bhat, R. N. and Ratnasamy, P.: *Zeolite*, **11**, 42 (1991).
11. Kim, G. J. and Kwon, L. M.: *HWAHAK KONGHAK*, **26**, 251 (1988).
12. Jacobs, P. A., Beyer, H. K. and Valyon, J.: *Zeolites*, **1**, 161 (1981).
13. Szostak, R. and Thomas, T. L.: *J. Chem. Soc. Chem. Commun.*, p. 113 (1986).
14. Derouane, E. E., Mestdagh, M. and Vielvoye, L.: *J. of Catal.*, **33**, 169 (1974).
15. Kumar, K., Thangaraj, A., Bhat, R. N. and Ratnasamy, P.: *Zeolites*, **10**, 85 (1990).
16. Borade, R. B.: *Zeolites*, **7**, 398 (1987).
17. Kuhl, G. H. and Schmitt, K. D.: *Zeolites*, **10**, 2 (1990).